SF 298 MASTER COPY KEEP THIS COPY FOR REPRODUCTION PURPOSES

REPORT DOCUMENTATION PAGE

Form Approved OMB NO. 0704-0188

1. AGENCY USE ONLY *(Leave blank)*	2. REPORT DATE	3. REPORT TYPE AND DATES COVERED
	Nov. 30, 2000	Final report, 01 Sep 96 - 31 Aug 00

4. TITLE AND SUBTITLE
Development of Microfabricated Radiation Sensor Systems

5. FUNDING NUMBERS
DAAH04-96-1-0418

6. AUTHOR(S)
W,K, Pitts, K.M. Walsh, and H.L. COx, Jr.

7. PERFORMING ORGANIZATION NAMES(S) AND ADDRESS(ES)
University of Louisville
Physics Department
Natural Science Building
Louisville, KY 40292

8. PERFORMING ORGANIZATION REPORT NUMBER

9. SPONSORING / MONITORING AGENCY NAME(S) AND ADDRESS(ES)
U.S. Army Research Office
P.O. Box 12211
Research Triangle Park, NC 27709-2211

10. SPONSORING / MONITORING AGENCY REPORT NUMBER
P-36362-RT-DPS.4

11. SUPPLEMENTARY NOTES
The views, opinions and/or findings contained in this report are those of the author(s) and should not be construed as an official Department of the Army position, policy or decision, unless so designated by other documentation.

12a. DISTRIBUTION / AVAILABILITY STATEMENT
Approved for public release; distribution unlimited.

12b. DISTRIBUTION CODE

13. ABSTRACT *(Maximum 200 words)*

This report is a description of the activity during 1996-1999 for the project "Development of MIcrofabricated Radiation Sensor SYstems". The project resulted in the the development of a new generation of radiation detectors and sensors, formed in thin polyimide with laser micromachining. These foils form both the mechanical support and insulating substrate, resulting in a thin, flexible, and ruggedized detector. During this project, sponsored activity included development of several new microfabricated gas proportional counters for radiation detection, development of techniques required to produce microstructuresin laser machined polyimide, development of a laser micro-fabrication facility at the University of LOuisville, development of techniques for post-machining cleaning and plating, operation of prototype detectors, studies of well geometry and its influence upon operation, and measurements with the CCD camera. Several papers reporting detector design and operation were published or will soon be submitted for publication. Five graduate students supported by this project received their degrees.

14. SUBJECT TERMS
Keywords: radiation detector, microfabrication, X-ray

15. NUMBER IF PAGES
7 plus appendices

16. PRICE CODE

17. SECURITY CLASSIFICATION OR REPORT	18. SECURITY CLASSIFICATION OF THIS PAGE	19. SECURITY CLASSIFICATION OF ABSTRACT	20. LIMITATION OF ABSTRACT
UNCLASSIFIED	UNCLASSIFIED	UNCLASSIFIED	UL

Development of Microfabricated Radiation Sensor Systems

Final Progress Report

U.S. Army Research Office

W.K. Pitts, K.M. Walsh, and H.L. Cox, Jr.
November 30, 2000

Grant DAAH04-96-1-0418

University of Louisville
Louisville, KY 40292

Approved for Public Release;
Distribution Unlimited

Table of Contents

Abstract

This final report is a description of the activity during 1996-1999 for the project "Development of Microfabricated Radiation Sensor Systems". The project resulted in the development of a new generation of radiation detectors and sensors, formed in thin polyimide with laser micromachining. These foils form both the mechanical support and insulating substrate, resulting in a thin, flexible, and ruggedized detector. During this project, sponsored activity included development of several new microfabricated gas proportional counters for radiation detection, development of techniques required to produce microstructures in laser machined polyimide, development of a laser microfabrication facility at the University of Louisville, development of techniques for post-machining cleaning and plating, operation of prototype detectors, studies of well geometry and its influence upon operation, and measurements with the CCD camera. Several papers reporting detector design and operation were published or will soon be submitted for publication. Five graduate students supported by this project received their degrees.

1: Introduction

This project developed low-cost, high performance radiation detection and X-ray imaging systems based upon microfabricated gas proportional chambers. The anticipated position resolution of approximately 50 microns allows their implementation into systems which are well suited to medical imaging, component inspection, monitoring of radioactive material, and law enforcement applications. An important advantage of the proposed system, compared to film-based systems, is that the data will be acquired in digital format. The required high density of readout elements will be achieved by using a CCD camera to record the light emitted during the electrical discharge of the detector. In these imaging applications, the detector functions as an image converter with gain.

During the period of this project (1996-2000), reliable techniques to produce microwell detectors have been fully developed, operational test results have been published, and first results from new designs are available. Since the best summary of the results have been published or are in press at this time, those publications are attached as appendices.

2: Scientific Progress and Accomplishments

2.1: Principles of Operation

The principles of operation were summarized in previous Annual Reports, and will be briefly described here. These detectors are miniaturized proportional counters, operating on the same physical principles as the familiar single wire and Multi-Wire Proportional Chambers (MWPC) [1,2]. All proportional chambers rely upon the secondary multiplication and amplification of the initial charge in a gas discharge. Free electrons, produced in a gas by ionizing radiation, drift to a region of intense electric field. Each electron will now be accelerated in the strong field, generating additional electrons through secondary ionization. The end result is an "avalanche" of electrons and photons at the anode. "Gas gain" is defined as the ratio of electrons collected at the anode to those produced by the initial ionizing event. Electrons are also produced at the cathode by several processes, such as positive ion recombination or photoemission caused by absorption of UV photons produced in the discharge. At a sufficiently high gas gain, the detector will continuously discharge as a result of this positive feedback mechanism. These undesirable feedback mechanisms are reduced or quenched by adding a second gas such as methane, which absorbs UV photons with subsequent reemission in the infrared region. Xenon has been demonstrated to have a quenching effect in argon/xenon mixtures.

Design details are presented more fully in earlier reports. A brief description of a microwell detector, illustrated in schematic form below, is that the active element is

formed as a well or via machined into metallized polyimide foil. The typical well dimensions are 100-200 micron diameter, fabricated in 125 micron thick Kapton© type H polyimide foil. Vias are spaced on a Cartesian grid of 200-400 micron spacing. A second cathode (the "drift electrode") element is placed 3-10 mm above the machined cathode plane. This electrode is biased to generate a low intensity electric field, such that the free electrons produced in the drift gap move toward the wells. Inside the well, charge multiplication occurs in the region of intense electric field generated between the upper cathode and lower anode surfaces.

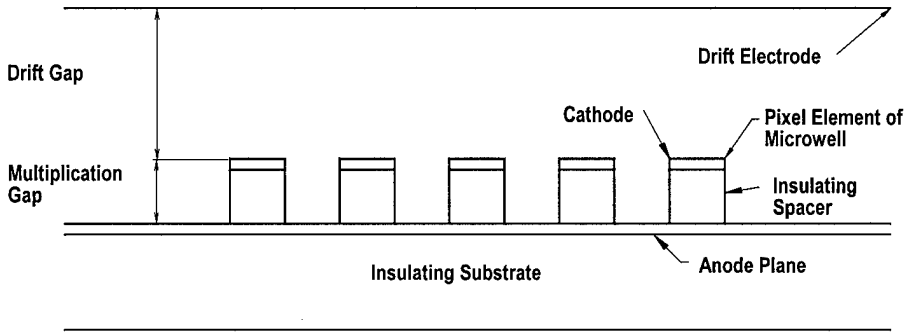

Figure 1: Schematic of the Microwell Detector Array.

At nearly the same time this device and its associated readout was disclosed for the patent process [3], similar detectors were proposed and developed in Europe [4,5]. The most developed concept is the GEM (Gas Electron Multiplier), produced at CERN by the Sauli group [5]. The GEM is an open channel through the substrate. In nearly all applications, the GEM is operated so that most of the electrons are not collected by the GEM anode but transported to an electrode below the GEM. Gas gains of up to 14,000 have been reported by CERN, and confirmed at other laboratories. Wet etching has been the fabrication technique of choice at CERN. An inevitable result of this chemical etching process is that the well tapers in from both sides, resulting in a conical ring of insulator in the center of the well. During operation, some fraction of the positive ions can be trapped on the polyimide surface protruding into the channel, resulting in short-term gain variations. Detectors fabricated with laser micromachining have straight sidewalls, and are less sensitive to short-term charging. This result was first proven in tests at the Lawrence Berkeley National Laboratory, with GEM detectors from CERN compared to GEM detectors from Louisville.[6] The elimination of short-term, rate dependent shifts may prove critical for applications with pulsed radiation sources, such as clinical X-ray imaging systems.

2.2: Final Process for MicroWell Detector Fabrication

Laser micromachining in air results in a tenacious layer of conductive residue attached to the polyimide surface. Continued development of the oxygen plasma etching process has

resulted in a reliable and efficient technique for producing detectors. A draft publication has been prepared containing relevant process parameters. This report is attached as Appendix C. After final revision, it will be submitted to *Nuclear Instruments and Methods in Physics Research.*

2.3: Operational Results with MicroWell Detectors

Operational results have been published in both *Nuclear Instruments and Methods* and *IEEE Transactions on Nuclear Science.* These papers are attached as Appendices A and B respectively.

2.4: The Microtube Detector

Described in last year's report, it is clear that a fundamental problem of most microstructure detectors is that is that the field lines tend to be along insulating substrates. Problems associated with the close presence of an insulating surface include charging as electrons and ions become attached to the surface and surface-associated electrical breakdown by surface streamer propagation. These effects may ultimately be responsible for the observed result that the product of rate and gas gain is approximately 10^8 for nearly all microfabricated detectors [10]. Only the microdot design, consisting of a circular anode within a cathode ring, surpassed this limit [11]. A new MWD design, with the anode reduced in area and extended into the well, would very likely have much improved performance compared to the standard MWD. Benefits should include higher gas gains due to the increased electric field, elimination of charging effects, and less likelihood of surface breakdown since the field lines are no longer parallel to the substrate. The breakdown path should be in the gas only, reducing the likelihood of damage to the substrate.[1]

Design calculations were presented in the 1998 report.

3: Supported Personnel, Publications, and Technology Transfer

3.1: Supported Personnel

Grant funds have been used to support Karl Pitts (Associate Professor, Physics) and Michael Martin (Research Technologist II, Physics). Graduate students (both M.S. and M. Eng.) have included Sylvia Matos (Physics),. Sergy Belolipetskiy (Physics and Electrical Engineering), Edward Sang (Electrical Engineering), and J.B.Hutchins

[1] Peskov has identified similar breakdown in the MicroStrip Gas Chamber as the origin of catastrophic failure [12].

(Electrical Engineering). All four supported students have received their Masters degree, along with Michael Martin. Several undergraduate students were supported in this project from a mix of grant funds and University funds.

3.2: Publications

The following papers have been published in refereed jounrals:

- "A Low-Cost, High Performance Cleanroom Enclosure", J.B. Hutchins, M.D. Martin, S. Belolipetskiy, H.L. Cox, Jr, W.K. Pitts, and K.M. Walsh. *IEEE Transactions on Education,* 42 144 (1999)
- "GEM: Performance and Aging Tests", H. Cho, J. Kadyk, S.H. Han, W.S. Hong, V. Perez-Mendez, W. Wenzel, K. Pitts, M.D. Martin, and J.B. Hutchins, *IEEE Transactions on Nuclear Science* 46 306 (1999)
- "Development and Operation of Laser Machined Microwell Detectors", W.K. Pitts, M.D. Martin, S. Belolipetskiy, M. Crain, J.B. Hutchins, S. Matos, J.H. Simrall, and K.M. Walsh, *Nuclear Instruments and Methods in Physics Research A438* 277 (1999) **(attached as Appendix A)**
- "Effect of Well Diameter upon MicroWell Detector Performance", W.K. Pitts, M.D. Martin, S. Belolipetskiy, M. Crain, J.B. Hutchins, S. Matos, J.H. Simrall, and K.M. Walsh, *IEEE Transactions on Nuclear Science* (in press) **(attached as Appendix B)**
- "Excimer Laser Microfabrication of Micropatterned Gas Proportional Counters", M.D. Martin, J.B. Hutchins, and W.K. Pitts *to be submitted to Nuclear Instruments and Methods in Physics Research* **(attached as Appendix C)**

3.3: Technology Transfer

No formal technology transfer was performed during this project. Results derived in the first two years of this project were reported to NASA/Goddard Spaceflight Center

4: Acknowledgements

Keith Solberg (Indiana University) developed and shared the initial concept for the microwell detector, and has furnished many insightful suggestions for detector fabrication and operation. Vladimir Peskov (NASA/Marshall Space Flight Center) and Fabio Sauli (CERN) were kind enough to discuss the superior performance of the microdot detector at high rates. John Kadyk (LBNL) offered many insightful comments upon the GEM in several extended discussions. Discussions with S.D. Hunter (NASA/GSFC), H.J. Crawford (LBNL), and P.V. Deines-Jones (NASA/GSFC) were useful in the course of this project.

References

[1] F. Sauli, *Principles of Operation of Multiwire Proportional and Drift Chambers*, CERN Report 77-09 (1977), reprinted in *Experimental Techniques in High Energy Physics*, Thomas Ferbel, editor; Addison-Wesley Publishing Company, Inc. (Menlo Park, California) 1987 (ISBN 0-201-11487-9)

[2] W. Blum and L. Rolandi, *Particle Detection with Drift Chambers*, Springer-Verlag (Berlin) 1993 (ISBN 0-387-56425-X)

[3] K. Solberg, W.K. Pitts, and K.M. Walsh, *Radiation Detector Based on Charge Amplification in a Gaseous Medium*, U.S. Patent 5,624,722, and W.K. Pitts, K.M. Walsh, and K. Solberg, *Optical Imaging System Utilizing a Charge Amplification Device*, U.S. Patent 5,602,397

[4] F. Bartol et al., Journal de Physique III (Paris) **6**, 337 (1996)

[5] R. Bouclier et al., *Nuclear Instruments and Methods in Physics Research* **A396**, 50 (1997); *IEEE Transactions on Nuclear Science* **NS-44**, 646 (1997); J. Benlloch et al., *Nuclear Instruments and Methods in Physics Research* **A419**, 410 (1998)

[6] H. Cho, J. Kadyk, S.H. Han, W.S. Hong, V. Perez-Mendez, W. Wenzel, K. Pitts, M.D. Martin, and J.B. Hutchins, *IEEE Transactions on Nuclear Science* 46 306 (1999)

[7] John B. Cooper et al., *Thin Solid Films* **303**, 180 (1997); M. Schumann, R. Sauerbrey, and M.C. Smayling, *Appl. Phys. Lett.* **58**, 428 (1991); T. Feurer, R. Sauerbrey, M.C. Smayling, and B.J. Story, *Appl. Phys. A* **56**, 275 (1993)

[8] TOSCA, Vector Fields, Ltd. (US Sales Office: Vector Fields, Inc., 1700 N. Farnsworth Avenue, Aurora, IL 60505

[9] E. Aprile, Columbia University, private communication

[10] V. Peskov, invited presentation at the *1998 IEEE Nuclear Science Symposium*, Toronto, Canada 1998; P. Fonte, V. Peskov, and B. Ramsay, *IEEE Transactions on Nuclear Science* 46 321 (1999)

[11] V. Peskov and F. Sauli, private commication

[12] V. Peskov et al., *Nuclear Instruments and Methods in Physics Research* **A392**, 89 (1997) ; V. Peskov et al., *Nuclear Instruments and Methods in Physics Research* **A397**, 243 (1997)

Appendix A: Development and Operation of Laser Machined Microwell Detectors (attached)

Appendix B: Effects of Well Diameter upon Micropatterned Gas Proportional Counters (attached)

Appendix C: Excimer Laser Microfabrication of Gas Microstructure Detectors (attached)

ELSEVIER

Nuclear Instruments and Methods in Physics Research A 438 (1999) 277–281

NUCLEAR INSTRUMENTS & METHODS IN PHYSICS RESEARCH Section A

www.elsevier.nl/locate/nima

Development and operation of laser machined microwell detectors

W.K. Pitts[a,*], M.D. Martin[a], S. Belolipetskiy[a,b], M. Crain[b], J.B. Hutchins[a,b], S. Matos[a], K.M. Walsh[b], K. Solberg[c]

[a]*Physics Department, Natural Science Building, University of Louisville, Louisville, KY 40205, USA*
[b]*Electrical Engineering Department, University of Louisville, Louisville, KY 40205, USA*
[c]*Indiana University Cyclotron Facility, Bloomington, IN 47408, USA*

Received 7 June 1999; received in revised form 16 July 1999; accepted 16 July 1999

Abstract

Arrays of 100 μm diameter cylindrical wells were laser micromachined on a 200 micrometer Cartesian grid, producing MicroWell Detectors (MWD). The substrate was 125 μm thick polyimide foil, more than twice as thick as a typical GEM or WELL detector. An advantage of the laser micromachining process is that the wells are produced with nearly vertical sidewalls, in contrast to the sloping sidewalls characteristic of conventional chemical etching processes. With the steeper sidewall, active elements may be more closely packed than is possible with wet etching techniques. Thicker substrates can be patterned, increasing the length of the charge multiplication region and reducing the internal capacitance per unit element. A series of prototypes have been produced and tested in a counting gas composed of 85% argon and 15% carbon dioxide, with a maximum measured gas gain of approximately 12 000.

PACS: 29.40.Cs; 29.40.Gx

Keywords: Detector; Proportional chamber; Micropatterned; GEM; WELL; CAT

1. Introduction

We report the application of laser micromachining to produce a MicroWell Detector (MWD), formed as an array of drilled 100 μm diameter cylindrical wells in 125 μm thick polyimide foil [1]. This detector is similar to the Compteur a Trou (CAT) [2,3], Gas Electron Multiplier (GEM) [4,5], WELL [6], and MicroGroove (MGD) [7] detectors, with an electrostatic field configuration similar to the MicroCAT design [8]. While each design differs in its arrangement of electrode and insulating substrate, a common feature is that secondary charge multiplication occurs in a cavity between planar electrodes. A further advantage of this field configuration, completely achieved in the GEM and WELL configurations, is that it can be easily produced in thin polyimide foils using inexpensive printed circuit technology. Laser

* Corresponding author. Tel.: + 1-502-852-0952; fax: + 1-502-852-0742.
E-mail address: kpitts@louisville.edu (W.K. Pitts)

0168-9002/99/$ - see front matter
PII: S0168-9002(99)00805-0

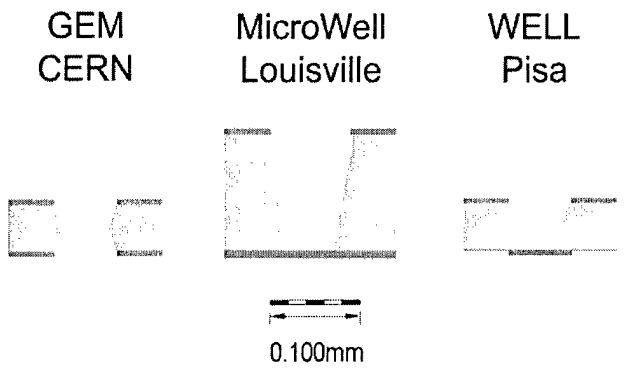

Fig. 1. Representative cross sections of the GEM, MicroWell, and WELL detector elements, drawn to scale.

microfabrication, however, allows a general and flexible control of detector geometry. The channels in the MWD, for example, are produced without the protrusions characteristic of wet etching. The differences are illustrated in Fig. 1, a scale drawing of the typical GEM, WELL, and MWD channels. Whether etched from either one side (WELL) or both (GEM), a wet-etched channel has a polyimide cone protruding into the channel. The laser machined channel more closely approaches an ideal cylindrical shape, with a wall sloping only 8° from the vertical. This steep wall angle allows smaller features to be packed more closely on thicker substrates. Applied to gas ionization detectors, for example, these techniques result in the ability to produce smaller active elements with reduced internal capacitance and a longer region of intense electric field.

The more cylindrical shape of the laser drilled channel also affects the operational characteristics of these detectors, demonstrated in a recent LBNL study of GEM devices [9]. A wet-etched GEM (furnished by CERN) had a +20% gain shift during the first hour of operation, probably due to avalanche ions collecting inside the GEM channel. A laser drilled GEM (produced in our laboratory) had a stable gain during the first hour of operation, presumably due to its more cylindrical channel without any protrusions.[1] The improved gain stability will be an important advantage for detector operation in an intense pulsed beam. This particular GEM was a prototype produced during development of effective post-machining cleaning techniques; more effective and more efficient techniques have since been developed to produce the MWD devices described in this report.

[1] Benlloch et al. also report similar conclusions concerning the shape of the GEM channel [4,5].

2. Detector fabrication

The MWD devices were fabricated using a combination of micromachining techniques developed for applications to microelectronics and microelectromechanical systems (MEMS). These techniques include excimer laser micromachining, post-processing cleaning, and nickel electroplating of patterned metal layers. A detailed technical report is being prepared [10]. Several combinations of well diameter and grid spacing were fabricated and tested, with most prototypes being arrays of either 200 μm diameter wells on a 400 μm Cartesian grid or arrays of 100 μm diameter wells spaced 200 μm apart on a Cartesian grid. Both thin (0.3 μm) and thick (5 μm) cathodes were fabricated. Detectors with 100 μm diameter wells and 5 μm thick cathodes gave the best performance, and those results are described in this paper. All detectors had active dimensions of 19.2 mm × 19.2 mm. The MWD cathodes were connected in parallel, while the MWD anode was a planar metal electrode. A drift cathode was mounted 11 mm above the detector plane. Detectors were baked overnight in the test chamber, at approximately 5×10^{-5} mbar pressure and 60°C temperature. Analysis of the vacuum with a residual gas analyzer showed little or no organic contamination at the end of the baking cycle. The anode/cathode resistance was approximately $10^{13}\Omega$, determined from the intrinsic MWD leakage current. The counting gas was 85% argon (99.999% purity) and 15% carbon dioxide (99.99% purity), delivered at a combined flow rate of 0.1 standard liters per minute. A solenoid valve regulated the chamber pressure at 931 mbar (700 Torr), controlled with feedback from an absolute capacitance manometer.

3. Test results

All detectors were tested with 5.95 keV X-rays from a ^{55}Fe source at a rate up to 100 Hz/mm^2. Pulses from either the MWD cathode or anode were processed with standard pulse counting electronics for nuclear spectroscopy, including a charge sensitive preamplifier (Tennelec TC174) and a spectroscopy amplifier with 3 μs shaping time constants. The gas gain was measured with two independent and absolute techniques. Direct measurements of the anode current were made with a calibrated picoammeter (Keithley 485), with the X-ray interaction rate determined by counting pulses from the cathode. The manufacturer's calibration of the picoammeter was verified using precision 1 and 10 GΩ resistors, biased by a constant voltage source to produce currents equivalent to those measured during the gas gain measurements. An alternative measurement of the gas gain relied upon calibration of the electronics chain with a known charge, injected into the preamplifier's input stage. Both methods agreed within the 10% systematic uncertainty of the charge injection technique.

Representative measurements are presented in Figs. 2 and 3. A pulse height spectrum at 12 000 gas gain is shown in Fig. 2. The sharp peak near channel 80 is the 37 fC charge input from the test pulser. A Gaussian was fitted to the full-energy peak, with a fitted full-width half-maximum (FWHM) of 17%

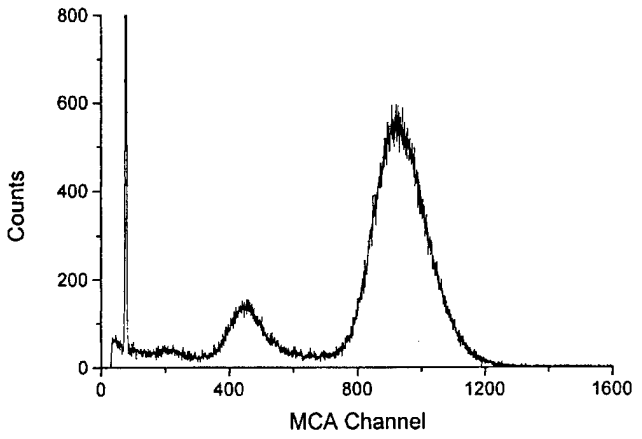

Fig. 2. Detector response to a ^{55}Fe source at a gas gain of 12 000. The sharp peak near channel 80 is the 37 fC pulser input.

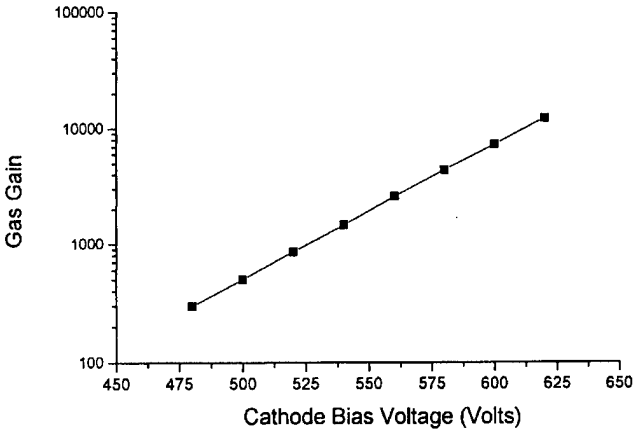

Fig. 3. Measured gas gain in a 85% argon, 15% carbon dioxide mixture. The MWD was an array of 100 μm wells on a 200 μm grid.

even at this high gas gain. The voltage dependence of the gas gain is shown in Fig. 3, with a maximum gas gain of approximately 12 000 at a drift field of 745 V/cm. There was little sensitivity to the drift field over a wide range of drift cathode bias voltages. Even though this MWD was as thick as two standard GEMs, shown to produce gas gains over 10^6 when operated in a cascaded system [4,5], the maximum gas gain was similar to that measured in many other micropatterned detectors. Both Ivaniouchenkov et al. and Bressan et al. have demonstrated that single micropatterned detectors are subject to Raether's criterion, breaking down at an avalanche size of a few 10^7 electrons [11,12]. During both experiments, a wide variety of detector configurations were tested. In almost all cases, the typical maximum gas gain of a single detector was limited to 15 000 or less. Higher gas gains and reduced sensitivity to sparking were achieved with a GEM preamplification stage, extending the conclusions reported in the original study of GEM preamplification structures operated above Multi Wire Proportional Chambers (MWPCs) and Micro Strip Gas Chambers (MSGC) [13].

In addition, Bellazzini et al. have now produced a combined GEM and MWD system [14]. The overall gas gain was measured as a function of the separation (transfer gap) between the GEM and MGD, each being 50 μm thick. In a high gain

neon–dimethyl ether (DME) mixture, the overall gas gain was as much as 300 000 with a 600 μm transfer gap. When the GEM was in direct contact with the MGD (zero transfer gap), the maximum gas gain was only 30 000. The proposed explanation is that larger transfer gaps furnish a region of field intensity sufficiently low that streamers from the anode become quenched and do not propagate to the cathode. Without a transfer gap, there is little or no quenching of streamers from the anode to the cathode. Similar considerations apply to the uniform field of the MWD, furnishing an implicit explanation for the gas gains reported in this paper. It may be, however, that the 125 μm thick MWD could achieve the same gas gains in a neon–DME counting gas mixture that have been reported for the GEM and MGD configuration with zero transfer gap.

4. Conclusions

Laser micromachining, a flexible and precise technology, has been applied to produce micropatterned detectors in polyimide foils. While this technology is more costly than conventional wet etching techniques, the ability to modify the active element geometry and associated operational characteristics make this technology well suited to develop specialized detectors capable of operating in an intense beam of X-rays, neutrons, or charged particles. Measured gas gains are comparable to those of other micropatterned detectors, presumably limited by the same breakdown mechanisms described in the literature [11–13]. Continued development will result in the ability to pattern 50 μm pixel elements, commensurate with the input pads of commercial imaging microelectronics. Forty micro meter diameter wells have already been drilled through 125 μm thick polyimide foils using the local facility. Further development of the MWD design will include an investigation of the optimum ratio of well diameter to substrate thickness, using 60, 100, 150, and 200 μm diameter wells in 125 μm thick polyimide. In addition, the gas gain will be measured in a neon–DME gas mixture optimized for high gain.

Acknowledgements

Discussions with Doug Bilodeau (IUCF), Hank Crawford (LBNL), Philip Deines-Jones (NASA/GSFC), Stan Hunter (NASA/GSFC), and John Kadyk (LBNL) were useful in the development of this new detector type. Jorge Moromisato (Northeastern University) furnished valuable details of his experience with laser micromachining of polyimide films. The E.I. duPont Company generously donated Kapton™ polyimide samples during the early phases of this project. Support from the DoD (Grant DAAH04-96-1-0418), NASA (Grant NAG5-5142), and the University of Louisville is gratefully acknowledged, as well as facility improvements sponsored by the National Science Foundation through the EPSCoR/ESI program. The National Science Foundation supports activity at the IUCF (Grant NSF PHY 96-02872 NUC RES).

References

[1] K. Solberg, W.K. Pitts, K.M. Walsh, United States Patent 5,614,722, 1997.
[2] F. Bartol, M. Bordessoule, G. Chaplier, M. Lemmonier, S. Megtert, J. Phys. III (France) 6 (1996) 337.
[3] G. Chaplier, J.P. Bouef, C. Bouillot, M. Lemmonier, S. Megtert, Nucl. Instr. and Meth. A 426 (1999) 339.
[4] F. Sauli, Nucl. Instr. and Meth. A 419 (1998) 189.
[5] J. Benlloch, A. Bressan, M. Capeans, M. Gruwe, M. Hoch, J.C. Labbe, A. Placci, L. Ropelewski, F. Sauli, Nucl. Instr. and Meth. A 419 (1998) 410.
[6] R. Bellazzini, M. Bozzo, A. Brez, G. Gariano, L. Latronico, N. Lumb, A. Papanestis, G. Spandre, M.M. Massai, R. Raffo, M.A. Spezziga, Nucl. Instr. and Meth. A 423 (1999) 125.
[7] R. Bellazzini, M. Bozzo, A. Brez, G. Gariano, L. Latronico, N. Lumb, A. Papanestis, G. Spandre, M.M. Massai, R. Raffo, M.A. Spezziga, Nucl. Instr. and Meth. A 424 (1999) 444.
[8] A. Sarvestani, H.J. Besch, M. Junk, W. Meissner, N. Pavel, N. Sauer, R. Stiehler, A.H. Walenta, R.H. Menk, Nucl. Instr. and Meth. A 419 (1998) 444.
[9] H.S. Cho, J. Kadyk, S.H. Han, W.S. Hong, V. Perez-Mendez, W. Wenzel, K. Pitts, M.D. Martin, and J.B. Hutchins, IEEE Trans. Nuc. Sci. 46 (3) (1999) 306.
[10] J.B. Hutchins, MSEE thesis, University of Louisville, 1999.
[11] Yu. Ivaniouchenkov, P. Fonte, V. Peskov, B.D. Ramsey, Nucl. Instr. and Meth. A 422 (1999) 300.
[12] A. Bressan, M. Hoch, P. Pagano, L. Ropelewski, F. Sauli, S. Biagi, A. Buzulutskov, M. Gruwe, G. De Lentdecker,

D. Moermann, A. Sharma, Nucl. Instr. and Meth. A 424 (1999) 321.

[13] R. Bouclier, W. Dominik, M. Hoch, J.-C. Labbe, G. Million, L. Ropelewski, F. Sauli, A. Sharma, G. Manzin, Nucl. Instr. and Meth. A 396 (1997) 50.

[14] R. Bellazzini, M. Bozzo, A. Brez, G. Gariano, L. Latronico, N. Lumb, M.M. Massai, A. Papanestis, R. Raffo, G. Spandre, M.A. Spezziga, Nucl. Instr. and Meth. A 425 (1999) 218.

Published in *IEEE Transactions on Nuclear Science, Vol. 47, No. 3, pp. 918-922, June 2000*

Effect of Well Diameter upon MicroWell Detector Performance

W.K. Pitts[1,2] , M.D. Martin[2], S. Belolipetskiy[2], M. Crain[3],
J.B. Hutchins[2], S. Matos[2], J.H. Simrall[2], and K.M. Walsh[3]
[2]University of Louisville, Physics Department, Louisville, KY 40205
[3]University of Louisville, Electrical Engineering Department, Louisville, KY 40205

Abstract

MicroWell (MWD) detectors have been produced by laser micromachining of 125 μm thick Kapton™ polyimide foil. Wells produced with this technique have near-vertical sidewalls with less than 10° of slope. It is an ideal tool to produce MWD prototype arrays with different well diameters for an experimental determination of the optimum ratio of well diameter to substrate thickness. Arrays with four different well diameters (60, 100, 150, and 180 μm) were machined into 125 μm thick Kapton™ polyimide foil. Detectors with well diameters commensurate with the substrate thickness had better performance, with the best design being an array of 150 μm diameter wells on a 200 μm Cartesian grid. This design achieved a gas gain of 17,000 in a counting gas of 70% argon and 30% carbon dioxide. Other significant advantages of this design included good charge collection from the drift region and increased gas gain with higher drift fields.

I. INTRODUCTION

The introduction of the Microstrip Gas Ghamber (MSGC) in 1988 led to a widespread effort to produce micropatterned gas proportional counters using techniques developed for the microelctronics industry [1]. These detectors promise the traditional advantages of proportional chambers, such as intrinsic gain, low cost, and radiation hardness, packaged into element sizes commensurate with applications such as particle tracking and X-ray imaging. Many of these promised advantages are being realized in designs such as the GEM (Gas Electron Multiplier) [2], the MWD (MicroWell Detector) [3], the WELL [4], the Microgroove [5], and the CAT (Compteur a Trou) [6]. Operational experience with a wide variety of these detectors, included a systematic study of maximum gas gains, has recently been published [7].

Optimizing a detector design such as the MWD requires varying a design feature over a series of prototypes. Consider the simple picture of the MWD as a well with a uniform electric field, with an electron lens above the well. A drift electrode is located well above the cathode, defining an active region where electrons produced by ionizing radiation drift to the well. An example of an idealized MWD is shown in Figure 1, with a 100 μm diameter well in a 200 μm square unit cell. This plot of the potential distribution (color code) and electric field lines (red lines) was calculated with the OPERA/TOSCA electrostatic analysis package [8]. Symmetric boundary conditions were imposed, modeling the effects of the other MWD elements on a regular Cartesian grid. Electric field lines are generated with the "flux tube" option of TOSCA. A bias voltage of –600V was applied to the perforated cathode, with a drift field of 3 kV/cm and a grounded anode. One important design variable is the well diameter, expressed as the aspect ratio (defined as the cathode-side well opening divided by the substrate thickness). An aspect ratio that is too small distorts the lens section of the field, leading to poor collection from the drift region. An aspect ratio that is too large will not concentrate the field in the well sufficiently for good gas gain. In addition, there will be some maximum voltage determined by the breakdown voltage along the wall of the well. Optimizing the gas gain for a given detector substrate becomes a question of optimizing the geometry, within the limits of a particular fabrication technology.

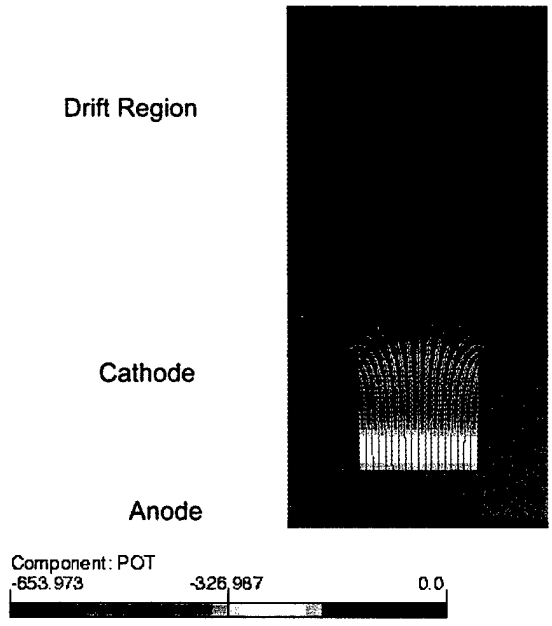

Figure 1: Electrostatic field calculation of a typical MWD, with 100 μm diameter wells on a 200 μm Cartesian grid.

One major advantage of the GEM, WELL, Microgroove, CAT, and MWD designs is that these designs may be fabricated using techniques developed for large-area flexible

[1]Research support from DoD grant DAAH04-96-1-0418, NASA grant NAG5-5142, and the University of Louisville.

printed circuit materials and multi-chip modules. Particular techniques include both wet chemical etching and laser micromachining. Laser machining is a commercially available technology used to produce patterned polyimide foils for integration into multi-chip modules and ink jet nozzles. A characteristic feature of laser micromachining is that the sidewall angle is very steep, being approximately 8° in the achieved MWD design. Chemical wet etching, however, results in sloping sidewalls approximately 45° to the vertical. The minimum pitch of a device produced with laser micromachining is not limited to approximately twice the substrate thickness, a general feature of devices produced by wet etching. In addition, a GEM or MWD array produced with laser microfabrication may be produced on a thicker substrate, significantly lowering the internal capacitance of the active element. Laser micromachining has proven to be an excellent technique for producing the MWD arrays required for an investigation of well geometry and its effect upon detector operation.

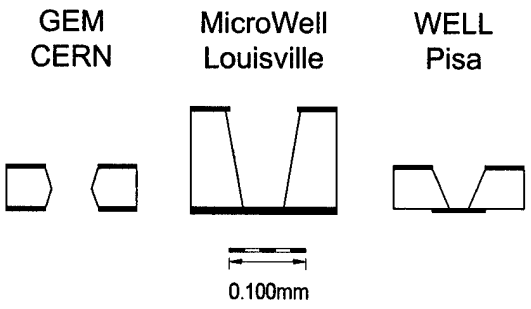

Figure 2: Cross sections of typical micropatterned detectors, drawn to scale.

Well geometry has been shown to have significant effects upon detector operation in the GEM configuration [9-10]. Consider the typical GEM, MWD, and WELL detectors, drawn to scale in Figure 2. One major difference between these three designs is that the standard GEM design has a protruding conical lip at the midpoint of the well, an inevitable feature of the wet chemical etching process. Positive ions produced in the channel of the GEM become attached to the protruding cone. This surface charge then distorts the electric field inside the well, leading to a reversible gain shift. In a comparison at LBNL, Cho et. al. have shown that laser machined GEM arrays produced in Louisville did not charge [9].

Detectors with five different MWD dimensions were fabricated for this study of the effects of aspect ratio (Table I). With the exception of the 150/400, several detectors of each type have been tested at this time. Well diameters were chosen to systematically vary the aspect ratio, with detector pitch chosen to be approximately twice the well diameter. One configuration (the 150/200) was produced with a much larger exposed anode area. All tested detectors had active dimensions of 1.9 ×1.9 cm^2 area. Four detectors were placed on a 100 mm diameter Kapton circle, a size compatible with the available fabrication equipment at the University of Louisville. Two of the four detectors were always the baseline 100/200 pattern, furnishing a check upon any processing problems.

Table 1
Well imensions of the MWD arrays, fabricated
In 125 μm thick Kapton foil

Label	Well Diameter (D)	Pitch (P)	Aspect Ratio (D/T)	Exposed Anode Area
60/100	60 μm	100 μm	0.48	28.8%
100/200	100 μm	200 μm	0.80	19.6%
150/200	150 μm	200 μm	1.200	44.2%
150/400	150 μm	400 μm	1.200	11.0%
180/400	180 μm	400 μm	1.44	15.9%

II. Detector Fabrication

The MWD devices were fabricated with excimer laser micromachining of 125 μm thick Kapton™ Type H polyimide foil. The typical wall angle was approximately 8° to the normal, with no polyimide protruding into the well or covering the anode. A reliable process to produce MWD arrays has been developed in our laboratory. Each process step is either commercially available or has a viable commercial replacement. The particular process steps are:

1. Sputter coat 125 μm thick Kapton Type H polyimide film with thin layers of chromium (10 nm) and gold (300 nm thick)
2. Laser ablate the thin metal layers for the MWD cathode pattern
3. Electroplate a 5 μm thick nickel layer onto the patterned gold layer, forming a conformal mask for the laser machining process
4. Ablate the polyimide foil in air, with intense patterned laser light
5. Remove carbonaceous residue with oxygen plasma processing.

A SEM photograph of the edge of a well is shown in Figure 3, after plating, laser ablation, and plasma processing. Note that the metal edge is clean, without damage from the laser machining process. An advantage of the conformal masking technique is that the laser beam may be projected using a slightly oversized mask, reducing the required alignment precision. A further benefit is that the intense laser beam smoothes and polishes the nickel electrode at the edge of the well where the electric field is most intense. The wall of the well shines brightly in the photograph, since electrons trapped on the highly resistive Kapton™ surface reflect the incident electron beam.

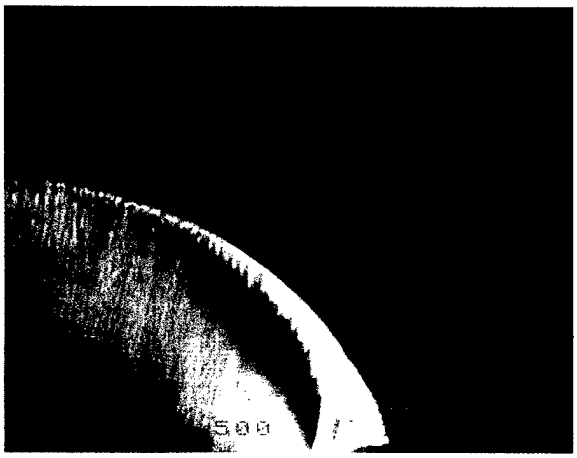

Figure 3: A typical segment of the cathode electrode and well at 500X magnification. Note the arc of polished nickel around the lip of the well.

In a given 1.9 × 1.9 cm^2 detector, all the MWD elements were connected in common. The typical resistance between the anode and cathode electrodes was approximately 10^{13} ohms, derived from measurements of the leakage current with applied bias voltage. Comparison to wet-etched GEM detectors of similar size shows that the surface resistivity is similar to that of wet-etched Kapton.

III. Test Procedures

Detectors were baked overnight in the test chamber, at approximately 10^{-5} mbar pressure and 60° C temperature. Analysis of the vacuum with a residual gas analyzer showed little or no organic contaminants present at the end of the baking cycle. The test chamber was filled with UHP grade argon and carbon dioxide. The manufacturer's cross-calibration of the flow controllers was verified using measurements of the pressure change with each gas stream.

The active region of the detector was defined by the planar cathode and an aluminum foil drift electrode 6.6 mm away. With the anode grounded, the cathode signal was detected and amplified in a Tennelec TC174 charge sensitive preamplifier and Tennelec TC248 spectroscopy amplifier (1.5 μs timing constants). Test pulses from a Ortec 419 pulser were injected into the preamplifier across its internal 1.2 pF test capacitor. Gas gains were derived from the measured response to the known charge input, compared to the photopeak of the 5.9 keV X-ray photon from a ^{55}Fe source [12]. Direct measurements of the anode current were made with a calibrated picoammeter (Keithley 485). Its calibration was verified with equivalent test currents, produced by biasing precision 1 GΩ and 10 GΩ resistors. The X-ray conversion rate was measured by counting cathode pulses.

Gas gains were measured in argon/carbon dioxide mixtures, either 85% Ar/15% CO_2 or 70% Ar/30% CO_2. While other gas mixtures such as neon-dimethyl ether or P-10 (90% argon/10% methane) will likely give a higher gain, the argon/carbon dioxide mixes are better for this systematic study. Comparison to the GEM research, for example, is much simpler using the same counting gas. A further advantage is that this gas mixture is described very well in the GARFIELD code for simulation of gas detectors [11]. Preliminary GARFIELD calculations are in very good agreement with previously measured MWD gains (Figure 4) [3].

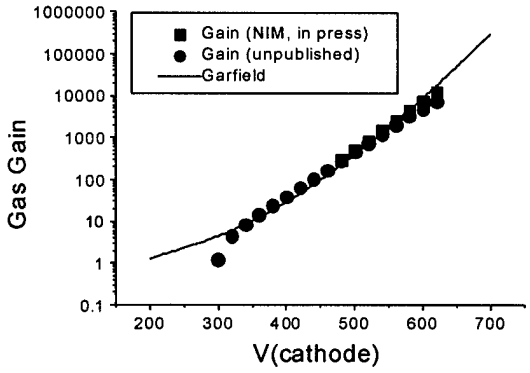

Figure 4: Comparison of GARFIELD calculations to a 100/200 MWD operated in 85% argon/15% carbon dioxide [3].

IV. Test Results

All the MWD arrays listed in Table I have been tested at this time, with the exception of the 150/400 design. It will be tested in the near future to complete this study. Both the 150/200 and 100/200 MWD designs had the best overall performance, giving high gain and good pulse height resolution. The 180/400 design had a lower gas gain at any given bias voltage, but could not be biased sufficiently to match the maximum gas gain of the 100/200 or 150/200 designs. In general, the 180/400 devices would break down at the same voltage as the 100/200 devices fabricated on the same 100 mm Kapton™ circle. A possible explanation, of course, is that the detector is breaking down along the sidewall in both detectors. None of the 60/100 devices operated in a satisfactory manner, having very poor spectra. The 100/200 test arrays fabricated on the same 100 mm circle operated successfully, however, with normal operating parameters. It is likely that the poor performance of the 60/100 devices is a real effect of an aspect ratio reduced below its optimum value.

Published in *IEEE Transactions on Nuclear Science, Vol. 47, No. 3, pp. 918-922, June 2000*

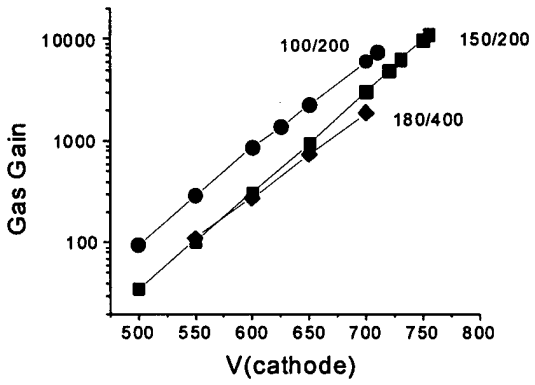

Figure 5: Measured gas gains for the tested MWD arrays for a –1.5 kV/cm drift field in a 70% argon/30% carbon dioxide gas mixture.

Comparative measurements of the gas gain for these three designs are shown in Figure 5. All these data were acquired at a relatively low drift field of –1.5 kV/cm, corresponding to –1 kV bias voltage on the drift electrode. These gas gains are measured after the detector has been operated at its respective bias voltage for approximately 30 minutes. This procedure more nearly approximates the "operational" conditions a detector would be expected to satisfy in an application. In addition, delaying the measurement of the gas gain allows the MWD array to charge. Charging typically resulted in a reversible gain drop of approximately 10-20%. The long-term charging is shown in Figure 6 for the 150/200 MWD operated at an initial gas gain of 3600. The X-ray rate was low, being only 10^4 Hz over the 3.6 cm^2 area of the detector. Similar charging effects were observed at higher gas gains.

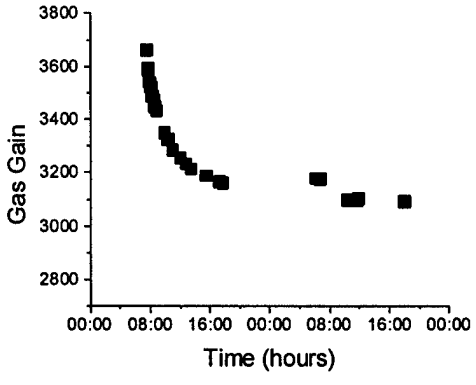

Figure 6: Charging of the 150/200 MWD arrays for a –1.5 kV/cm drift field in a 70% argon/30% carbon dioxide gas mixture.

The collection efficiency of the 150/200 MWD was very good (Figure 7) , presumably due to the large open area (44%) of the wells. Note that full collection occurs even at relatively low applied voltages, which may allow a 150/200 MWD to be operated in a fast gated mode. In this mode, sending a fast, high voltage pulse to the drift electrode would turn the detector on. A similar trend was observed in the 100/200 MWD array, although higher voltages were required to fully collect electrons from the drift region.

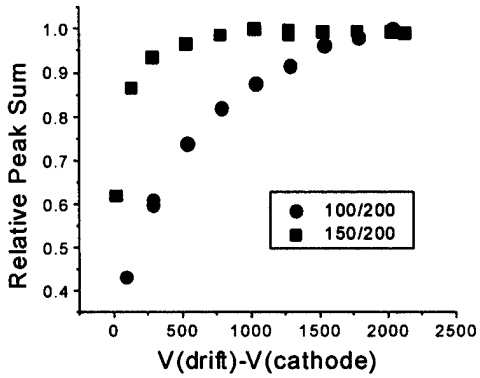

Figure 7: Variation of the collection efficiency with drift voltage for the 100/200 and 150/200 MWD arrays

An unexpected result was that the gas gain of the 150/200 design in the 70% argon /30% carbon dioxide gas mixture increased with drift field until the drift electrode would spark (Figure 8). This behavior is not seen in the 100/200 design, for example, which has a maximum and then decreases. This increase in gain with drift field is likely due to the 150/200 MWD having a large fraction (44%) of its anode open to the drift field. In addition to reducing the area of the cathode that can sink field lines, the electrostatic field lens extends further into the drift region.

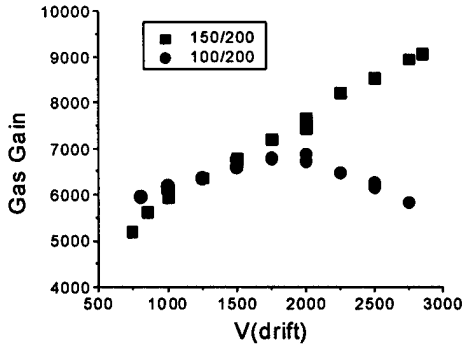

Figure 8: Variation of the gas gain with drift voltage.

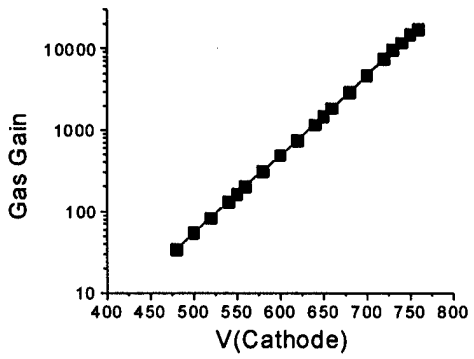

Figure 9: Gas gain of the 150/200 MWD, measured under ideal conditions.

An interesting feature of these measurements is that the maximum gas gain of the 150/200 design is much higher at higher drift field (Figure 9). During this test, the drift field was 3 kV/cm and the gas gain was measured immediately after ramping the cathode bias voltage. Under these circumstances, the maximum gas gain was 17,000. Charging would be expected to reduce this by approximately 15%. A sample spectrum at 17,000 gas gain and 1.5 μ sec shaping time is shown in Figure 10. The FWHM (full-width at half maximum) of the photopeak is 25%, even at this high gain. In general, the FWHM at lower gas gains (e.g. 10,000 or lower) was less than 20%. Spectra quality is an important test of MWD quality. Wells with differing gain result in widening of the photopeak and filling the area between the photopeak and the fluorescence peak at 3 keV. The small peak at approximately 1.3 keV is likely due to fluorescence X-rays emitted from the thick aluminum foil of the drift electrode.

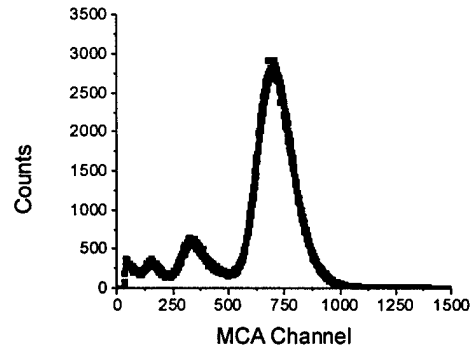

Figure 10: Detector response to 5.9 keV X-rays at 17,000 gas gain.

V. Future Plans

Testing the 150/400 MWD is required to finish this study of aspect ratio and its effect upon detector performance. With those test results, it will be possible to determine if the good performance of the 150/200 MWD is due to the aspect ratio, pitch, or combination of the two. Extension of the 150/200 design to the GEM design is a high priority, due to the open area of this MWD array. The combination of open structure and cylindrical well should result in a GEM with excellent electron transmission and no charging dependent gain shifts.

VI. Acknowledgements

During this project, K. Solberg (IUCF), Dr. J. Kadyk (LBNL), R. Srinivasan (UV Tech Associates), Dr. H.J. Crawford (LBNL), Dr. P.V. Deines-Jones (NASA), and Dr. S.D. Hunter (NASA) furnished suggestions for detector fabrication and operation. E.I. DuPont furnished Kapton™ samples.

VII. References

[1] A. Oed, "Position-sensitive detector with microstrip anode for electron multiplication with gases", *Nucl. Instrum. and Meth. A*263, pp. 351-359, 1988

[2] F. Sauli, "GEM: A New Concept for Electron Amplification in Gas Detector", *Nucl. Instrum. and Meth. A*386, pp. 531, 1997.

[2] W.K. Pitts et al., "Development and Operation of Laser Machined MicroWell Detectors", *Nucl. Instrum. and Meth. A* (in press)

[4] R. Bellazzini et al., "The WELL Detector," *Nucl. Instrum. and Meth. A*423, pp. 125-134, 1999.

[5] R. Bellazzini et al., "The Micro-groove Detector," *Nucl. Instrum. and Meth. A*424, pp. 444-458, 1999.

[6] F. Bartol et al., "The CAT Pixel Proportional Gas Counter Detector", *J. Phys. III (France)* 6 pp. 337-347, 1996.

[7] A. Bressan et al., "High Rate Behavior and Discharge Limits in Micro-Pattern Detectors," *Nucl. Instrum. and Meth. A*424, pp. 321-342, 1999.

[8] Vector Fields, Inc. 1700 N. Farnsworth Ave., Aurora, IL 60505

[9] H.S. Cho et al., "GEM: Performance and Aging Tests", *IEEE Trans. Nucl. Sci.* 46, (1999) 306-311.

[10] J. Benlloch et al., "Further developments and beam tests of the gas electron multiplier (GEM)", *Nucl. Instrum. and Meth. A* 419, pp. 410-417, 1998.

[11] R. Veenhoof, "GARFIELD, recent developments", *Nucl. Instrum. and Meth. A*419, pp. 726-730, 1998.

[12] Z. Ye et al., "Gas Amplification in High Pressure Proportional Counters", *Nucl. Instrum. and Meth. A*329, pp.140-150, 1993

To be submitted to Nuclear Instruments and Methods in Physics Research

Excimer Laser Microfabrication of Micropatterned Gas Proportional Counters

M.D. Martin, J.B. Hutchins, and W.K. Pitts[1]
University of Louisville, Physics Department,
Louisville, KY 40292

Laser microfabrication, a technique suitable for producing precisely machined structures in polyimide foils, has been applied to the production of micropatterned gas proportional counters such as the MicroWell Detector (MWD) and the Gas Electron Multiplier (GEM). Techniques have been developed to produce microstructures that have a high vertical relief in a 125 μm thick polyimide substrate, excellent metal electrodes, steep vertical sidewalls, high resistivity polyimide surfaces, and lower capacitance than devices produced with other techniques. Detectors produced with these techniques have been operated with gas gains comparable to other micropatterned gas proportional counters such as the GEM. We also report on the effect of laser machining parameters, such as fluence (energy/unit area) and pulse repetition rate, upon the final device. Commercially available equivalent processes for production of large area devices are specified.

1. Introduction

We report on the application and further development of excimer laser microfabrication to the production of micropatterned gas proportional counters. Much of the current interest in micropatterned gas proportional counters such as the Microwell Detector (MWD) [1-3], the Gas Electron Multiplier (GEM) [4-5], the Compter a Trou (CAT) [6-7], WELL [8], Microgroove [9], MicroCat [10-11], MICROMEGAS [12-13], and Micro Pin Array Detector (MIPA) [14] detectors is due to their general suitability for high rate, positive sensitive particle detection using inexpensive production techniques. Sauli and Sharma have recently published an extensive overview of the wide variety of micropatterned gaseous detectors [15].

A general feature of many of these detectors is that charge multiplication and gas gain occurs in an enclosed channel or well, machined from one side of the substrate to another. In the case of the MWD, WELL, and CAT designs, the channel is closed at its bottom with a planar anode. The GEM has an open channel, with both the anode and cathode being a circular opening at the entrance and exit of the well. While many of the different variants of these counters have been produced with standard wet chemical etching, laser micromachining offers significant advantages and a wider range of options compared to conventional techniques. One particular advantage is that detectors may be produced on thicker substrates, reducing the overall detector capacitance and significantly improving the overall signal to noise of a detector system. MicroWell Detectors (MWD) and Gas Electron Multiplier (GEM) devices have been produced with these techniques in our laboratory and reported in earlier publications [1-2,16]. This report contains a more detailed description of the laser micromachining

[1] Corresponding author, present address: Pacific Northwest National Laboratory, MSIN P8-08, P.O. Box 999, Richland, WA 99352; e-mail karl.pitts@pnl.gov

techniques developed to produce the MWD. Equivalent specifications for commercially available processes are also discussed.

The laser drilling process offers several advantages over typical wet etching. Laser drilled wells are much closer to the idealized cylindrical geometry than those formed with by chemical wet etching. Laser machined features may be produced at a pitch much smaller than the substrate thickness. It could be used to produce detector arrays in assembled multi-layered polyimide circuit boards. A final advantage is that the precise removal of material in all 3 dimensions allows the fabrication of novel, complex structures that would be difficult to produce using other techniques. The structure in Figure 1 demonstrates the flexibility of this technique. After machining a combination of different diameter wells to different depths on a common center, a final cut opened up the wells to a common centerline. This type of shape is impossible to form with chemical wet etching.

Stable detector operation at high gas gain requires that the detectors have smooth electrode edges to reduce electron field emission at the cathode, high resistivity substrates along the sidewall to reduce charging, and uniform machining from well to well. These requirements are met in our devices using a combination of laser patterning, electroplating, polyimide machining, and post-processing cleaning. The major process steps are:

1. Machine the electrode pattern in a thin (0.3 μm) gold or copper layer bonded to a polyimide foil with a thin (0.01μm) chromium layer
2. Electroplate the electrode pattern with a 5 μm thick nickel layer
3. Laser machine the wells in the polyimide material of the substrate
4. Remove polyimide debris using oxygen plasma ashing.

Each step is described below in more detail, including relevant details of commercially available equivalent processes.

2. Laser Ablation of Polyimide

Excimer laser ablation of polyimide is a tool developed for the microelectronics industry and materials processing. Its unique combination of high aspect ratio, high material removal rates, and edge resolution of 2-3 μm makes it an attractive technology for forming wells and channels in polyimide [17-18]. The UV light from the laser is readily absorbed in the first few hundred nanometers of the substrate, breaking down the polyimide through a combination of thermal and photochemical decomposition. Reaction products ejected from the surface at high temperatures and supersonic speeds. Extensive modeling and dedicated experiments confirm this picture [19]. In addition, there is an extensive literature reported details of the machining process [20-22].

Metal layers 0.1-0.6 μm thick deposited on polyimide are also effectively patterned with excimer laser ablation. If the metal layer is not too thick, sufficient heat is transferred to ablate the underlying polyimide underneath the hot metal film. The metal film expands outward, rupturing if the initial fluence (areal energy density of a single laser pulse at the working

surface) is sufficiently high. If the fluence is sufficiently high, then the film is entirely removed over the illuminated region, in a fashion similar to the "lift off" photolithographic process. Single laser shots at differing fluences were used to pattern 60 μm diameter circles in a 0.1 μm thick copper layer deposited on a 25 μm thick polyimide film (Figure 2). The edge quality increases with increasing fluence and heating of the metal layer. Depending on the particular application, copper or gold layers 0.1–0.4 μm thick are suitable for direct laser patterning.

Despite an intensive development effort, direct microfabrication of MWD devices with thin (0.1-0.4 μm) metal layers is not a viable, high-yield production process. The cathode edge is damaged during machining the well, as ablation products ejected at supersonic speed tear the overhanging thin metal edge and attack the underlying polyimide at the lip of the well. Plating the thin metal cathode with a 5 μm thick nickel layer, however, results in a metal layer that is mechanically robust. In addition, nickel films this thick will withstand direct exposure to thousands of laser pulses without damage. Forming the cathode in this material gives a thick electrode that may be used as a conformal mask, resulting in exact registration between the cathode opening and the well. Figure 3 shows a portion of a well produced with the conformal mask technique. Although the fluence is too low to ablate the nickel layer, it still partially melts and polishes the metal at the edge of the well. Smoothing the metal edge reduces the localized high electric fields at the edge of the cathode, reducing the field emission of electrons from the cathode. In addition, forming the anode of the MWD as a 5-10 μm thick nickel layer gives a stop layer for the laser beam and eliminates the need for precise depth control.

A characteristic feature of laser micromachining is that the walls are very steep in comparison to those formed with chemical wet etching (e.g. Figure 1). Increasing the fluence increases the wall angle, up to a geometry dependent limit reached at a fluence between 800 and 1000 mJ/cm^2 [23]. Representative measurements with the University of Louisville system are shown in Figure 4. The typical fluence during MWD fabrication was 800-900 mJ/cm^2, resulting in typical wall angles of 82°-84°.

Once a MWD or GEM has been laser machined in air, it is necessary to remove the highly conductive residue of thermally decomposed polyimide. On the planar surface of the cathode, there is a grainy carbonaceous residue deposit. Along the sidewall of the well, there is a highly conductive layer that seems to be a carbonaceous residue deposited on a layer of conductive, thermally decomposed polyimide. Cleaning techniques that effectively removed the surface deposits on the cathode did not affect this layer along the sidewall. One possible explanation for the different properties of these two residues is that hot ablation products sticking to a hot organic sidewall produce the extremely tenacious sidewall deposits. The underlying layer is most likely formed by repeated exposure to low-intensity laser light at the side of the well, a mechanism known to produce surface layers of high conductivity [24-27]. Comparing wells machined at low (10 Hz) and high (100 Hz) repetition rates showed that the conductivity depends strongly upon pulse rate, indicating that thermal damage of the underlying polyimide is also important. The supported data are described in detail below.

3. Post-Processing Cleaning

Both wet chemical and dry plasma processes were developed to clean the residue. A successful wet chemical process would easily scale to large areas and require no specialized processing equipment. A dry plasma process, however, would be compatible with a much wider variety of electrode metals, but require specialized processing equipment. The graphitic carbon on the metallic cathode is removed with ultrasonic cleaning in a variety of chemical baths. Organic solvents such as trichloroethylene (TCE) or a 5:1 mixture of deionized water and 5% sodium hypochlorite solution (household bleach) are relatively effective at cleaning the surface. The only effective chemical agents that removed the wall deposits were the diluted sodium or calcium hypochlorite solutions. Ultrasonic agitation after soaking in a 50° C solution for 1-2 hours removed the wall deposits. While an effective technique to clean polyimide, these solutions were not compatible with the metal layers required for the cathode. Both nickel and copper were aggressively attacked. Even gold layers were difficult to fabricate, with the chromium adhesion layer between the gold and polyimide attacked by crevice corrosion in the hypochlorite solutions.

A process that efficiently removes the entire residue without damaging the metal electrodes is oxygen plasma ashing. Pure oxygen at low pressure is dissociated to produce oxygen atoms that aggressively react with the carbonaceous residue. If the plasma reactor was operated at lower gas pressure and higher RF dissociator power, producing a higher proportion of oxygen ions, then the cleaning was not as effective. Optimum operating parameters were determined using measured MWD leakage currents (Figure 5). Measurements at low voltage, e.g. measurements with standard laboratory ohmmeters, overestimate the resistance and quality of the surface resistivity. Note that there is a broad minimum in the resistivity as a function of exposure, and that overexposure increases conductivity. The ability to adjust the sidewall conductivity may be useful in the reduction of charging effects and associated gain shifts in the MWD and GEM geometries at high rates.

The laser repetition significantly affects the quality of the resulting sidewall. Since machining speed is linearly related to repetition rate, the most efficient machining technique is to operate the laser at moderate power and high rate. The resulting residue is significantly more conductive than that formed at lower repetition rates. This qualitative impression was confirmed by comparing the resistance of a MWD array machined at a repetition rate of 10 Hz to one machined at 100 Hz, as a function of exposure time to the oxygen plasma cleaning process (Figure 6). Slower machining rates resulted in improved sidewall resistivity. This trend is consistent with the underlying picture of substrate damage due to heat flow; machining at high repetition rate does not allow sufficient time for the substrate to cool before the next laser pulse.

4. Summary of the MWD and GEM Fabrication Process

A standard layout for detector prototypes was 4 individual detectors fabricated on a 100 mm diameter circle of 50, 75, or 125 μm nominal thickness type H Kapton™ polyimide foil [28]. The MWD arrays were typically glued to 100 mm diameter glass discs for ease of handling.

This geometry matches the 4" wafer microfabrication equipment in the Lutz Microfabrication Facility at the University of Louisville. Available processes and diagnostic tools include the availability of many different sputtered metal coatings, dry plasma processing, wafer dicing saws, wire bonders, and diagnostic tools. Each step in the detector fabrication process is described in more detail below.

The polyimide circles were metallized after cleaning in isopropanol, methanol, and acetone. After cleaning the circles were baked at 200°C in a vacuum oven for 1 hour. Baking dehydrates and shrinks the sample, improving metal adhesion and dimensional stability [28]. A 0.01μm chromium layer is sputtered on the polyimide film, followed immediately by the sputtering of a 0.3 μm thick gold layer.

The cathode and anode layers are patterned with the laser, cleaned for 10 minutes with oxygen plasma ashing, and electroplated with a nominal 5 μm thick nickel layer. The nickel plating solution is a low-stress nickel sulfamate bath [29]. Adding approximately 0.5 g/l of sodium dodecyl sulfate, a wetting agent, were added for better coverage.

After electroplating, the wells are laser drilled using the nickel-plated cathode as a conformal mask. The usual practice is to use a mask with the projected spots being 20-50% larger than the well opening of the cathode. With the larger spot, the alignment tolerances are relaxed and a laser polished rim is produced at the surface of the well. The usual machining parameters for machining a 125 μm thick MWD are 600-700 laser pulses at a fluence of 800-900 mJ/cm^2 and a repetition rate of 100 Hz.

After machining the MWD devices are cleaned in the oxygen ashing plasma for 30-60 minutes, depending on the geometry. GEM detectors have 5μm of Ni plated on to the anode after 30-60 minutes of ashing with the above parameters before they are operated.

5. Commercially Available Equivalent Processes

Large-scale laser micromachining of MWD and GEM detectors is feasible using commercially available processes, if each step of the process is selected with an understanding of the underlying engineering aspects. A collection of recommended procedures includes:

- Patterned electrodes are available from a wide variety of commercial vendors. The cathode, for example, may be produced in a 5 μm thick copper layer as a standard flexible printed circuit. Depending upon the oxygen plasma ashing process, it may be necessary to protect the copper layer with a nickel or gold plating. All results in this paper were obtained with "adhesiveless" material, with a layer of chromium bonding the metal to the polyimide. No tests were made with material in which the metal films are glued to the polyimide. This material was judged incompatible with long term operation, since volatile products from the glue layer could possibly poison the counting gas.
- Oxygen plasma ashing is a standard microelectronics technique, available in a wide variety of reactors and processes. Many reactors will accept pieces 20 × 20 cm^2 or larger. While the process parameters must be determined for each reactor,

measurements of the leakage current are an excellent diagnostic tool. As mentioned above, measurements of the resistance at low voltage are not adequate.

- Laser machining is available at many vendors, with a variety of lasers. The standard commercial process for high quality polyimide machining uses excimer lasers emitting at either 197, 248, or 308 nm. Other processes may give equally acceptable results but have not been tested. Designing the cathode to be a conformal mask simplifies the machining process, reducing the required alignment tolerance.
- Specifying the laser machining parameters has a significant impact upon further processing steps. Polyimide machined at low repetition rates is easier to clean than that machined at high rates, for example, and this particular parameter must be specified.

It is clear that commercial production of laser micromachined MWD and GEM detectors is viable if the required processes are carefully specified.

6. Conclusions and Future Directions

We have successfully produced laser machined MWD detector arrays that have been operated with gas gains over 15,000 in a gas mix of 70% argon and 30% carbon dioxide [1-2]. Fabrication details are furnished in this report, including suggestions for commercially equivalent processes. Further research is in progress to develop new types of gas microstructure detectors, taking advantage of the unique capabilities of laser processing. Compared to wet etching, laser machined detectors can be produced with lower capacitance per unit element, an important consideration in producing low noise detector systems. Other work in progress is the development of electrodes of different shape. Combined with electroforming techniques, these techniques may be used to produce detectors with new electrode designs. These new devices are now being tested and will be presented in a future report.

Acknowledgements

Many individuals furnished advice for the development of these techniques, with the contributions of S. Belolipetskiy (University of Louisville), M. Crain (UofL), S. Matos (UofL), H. Simrall (UofL), K. Solberg (Indiana University Cyclotron Facility), R. Srinivasan (UV Tech Associates), and K.M. Walsh (UofL) being especially noteworthy. Discussions with H.J. Crawford (Lawrence Berkeley National Laboratory), P.V. Deines-Jones (NASA/Goddard Space Flight Center), S.D. Hunter (NASA/GSFC), V. Peskov (NASA/Marshall Space Flight Center) and J. Kadyk (LBNL) were useful in the development of this new detector type. M. McAlees of E.I. DuPont furnished a wide variety of Kapton™ samples for this project. Support from the DoD (Grant DAAH04-96-1-0418), NASA (Grant NAG5-5142), and the University of Louisville is gratefully acknowledged, as well as facility improvements sponsored by the National Science Foundation through the EPSCoR/ESI program.

References:

[1] W.K. Pitts, M.D. Martin, S. Belolipetskiy, M. Crain, J.B. Hutchins, S. Matos, K.M. Walsh, and K. Solberg, *Nucl. Instr. and Meth.* A 438, 277 (1999)
[2] W.K. Pitts, M.D. Martin, S. Belolipetskiy, M. Crain, J.B. Hutchins, S. Matos, J.H. Simrall, and K.M. Walsh, *IEEE Trans. Nucl. Sci. 47* (2000) 918
[3] P.V. Deines-Jones, K. Black, S.D. Hunter, and H.J. Crawford, to appear in *Proceedings of the Fifth International Conference on Position Sensitive Detectors,* September 1999, London, England
[4] F. Sauli, *Nucl. Instr. and Meth.* A 386, 531 (1997)
[5] J. Belloch, A. Bressan, et al., Nucl. Instr. and Meth. A419 (1998) 410
[6] F. Bartol, M. Bordessoule, G. Chaplier, M. Lemmonier, and S. Megtert, *J. Phys. III (France)* 6 (1996) 337,
[7] G. Chaplier, J.P. Bouef, C. Bouillot, M. Lemmonier, and S. Megtert, *Nucl. Instr. and Meth. A* 426 (1999) 339
[8] R. Bellazzini, M. Bozzo, A. Brez, G. Gariano, L. Latronico, N. Lumb, A. Papanestis, G. Spandre, M.M. Massai, R. Raffo, and M.A. Spezziga, *Nucl. Instr. and Meth. A* 423 (1999) 125
[9] R. Bellazzini, M. Bozzo, A. Brez, G. Gariano, L. Latronico, N. Lumb, A. Papanestis, G. Spandre, M.M. Massai, R. Raffo, and M.A. Spezziga, *Nucl. Instr. and Meth. A* 424 (1999) 444
[10] A. Sarvestani, H.J. Besch, M. Junk, W. Meissner, N. Sauer, R. Stiehler, A.H. Walenta, and R.H. Menk, *Nucl. Instr. and Meth. A* 410 (1998) 238
[11] A. Sarvestani, H.J. Besch, M. Junk, W. Meissner, N. Pavel, N. Sauer, R. Stiehler, A.H. Walenta, and R.H. Menk, *Nucl. Instr. and Meth. A* 419 (1998) 444
[12] Y. Giomataris, Ph. Rebourgeard, J.P. Robert, and G. Charpak, *Nucl. Instr. and Meth. A* 376 (1996) 29
[13] G. Barouch et al., *Nucl. Instr. and Meth. A* 423 (1999) 32
[14] P. Rehak, G.C. Smith, J.B. Warren, and B. Yu, *IEEE Trans. Nucl. Sci. 47* (2000) 1426
[15] F. Sauli and A. Sharma, *Ann. Rev. Nucl. Part. Sci. 49* (1999) 341
[16] H.S. Cho, J. Kadyk, S.H. Han, W.S. Hong, V. Perez-Mendez, W. Wenzel, K. Pitts, M.D. Martin, and J.B. Hutchins, , *IEEE Trans. Nucl. Sci. 46* (1999) 306-311
[17] W.W. Duley, *UV Lasers: Effects and Applications in Material Science,* Cambridge University Press, 1996, ISBN 0521464986
[18] *Laser Ablation: Mechanism and Applications II,* John C. Miller and David Geohegan, editors, AIP Conference Proceeding Series Number 228, AIP, ISBN 1563962268
[19] H. Schmidt, J. Ihlemann, B. Wolff-Rottke, K. Luther, and J. Troe, *J. Appl. Phys.* 83, 5458 (1998)
[20] V.P. Veiko, S.M. Metev, A.I. Kaidanov, M.N. Libenson, and E.B. Jakovlev, *J. Phys. D. 13* (1980) 1565
[21] V.P. Veiko, S.M. Metev, K.V. Stamenov, H.A. Kalev, B.M. Jurkevitch, and I.M. Karpman, *J. Phys. D. 13*, (1980) 1571
[22] T.W. Hodapp and P.R. Fleming, *J. Appl. Phys. 84* (1998) 577
[23] X. Zhang, S.S. Chu, J.R. Ho, and C.P. Grigoropoulos, *Appl. Phys. A 64* (1997) 545
[24] R. Srinivasan, R.R. Hall, W.D. Loehle, W.D. Wilson, and D.C. Allbee, *J. Appl. Phys. 78* (1995) 4881
[25] H.M. Phillips, S. Wahl, and R. Sauerbrey, *Appl. Phys. Lett. 62* (1993) 2572
[26] T. Feurer, R. Sauerbrey, M.C. Smayling, and B.J. Story, *Appl. Phys. A 56* (1993) 275
[27] M. Schumann, R. Sauerbrey, and M.C. Smayling, *Appl. Phys. Lett. 58* (1991) 428

[28] Kapton™ is a registered trademark of DuPont, Inc. A technical summary of the properties of Kapton™ is available from DuPont, Circleville, OH
[29] *Modern Electroplating*, by the Electrochemical Societry, Frederick A. Lowenheim, ed. John Wiley and Sons, NY ISBN 047154968

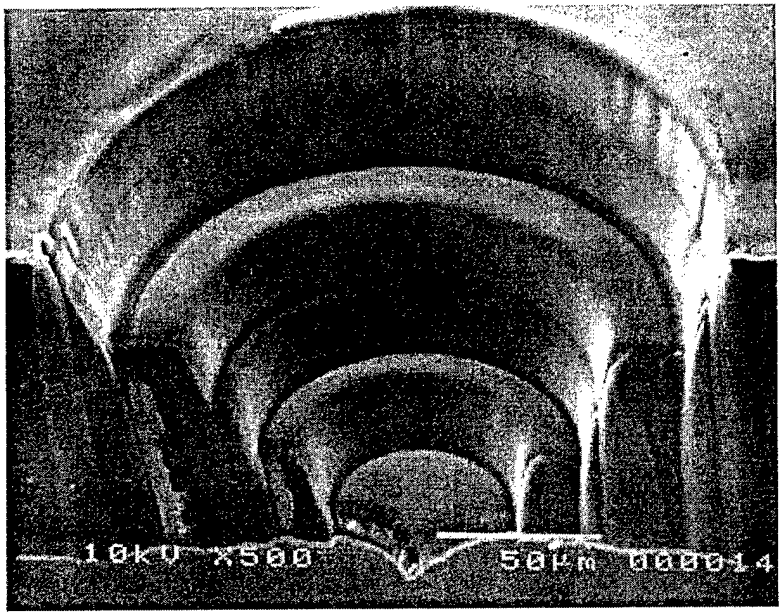

Figure 1: A laser micromachined structure, formed by sequential drilling of 200, 180, 120, 100, and 60 µm diameter wells in 125 µm thick polyimide followed by a cross section cut with the laser.

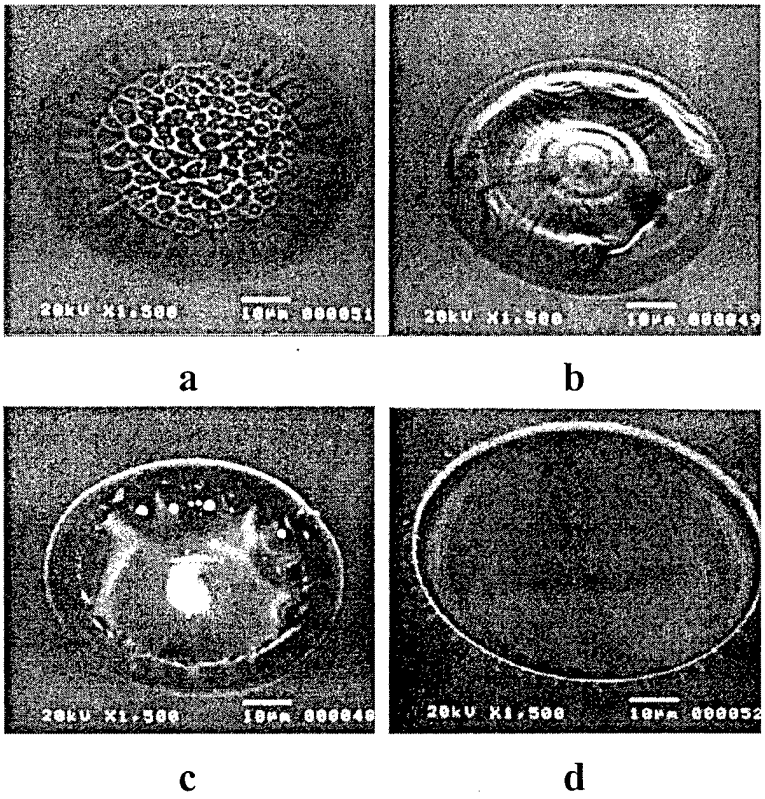

Figure 2: Direct laser patterning of 0.1 μm thick copper layers on polyimide, at (a) 370 mJ/cm^2, (b) 400 mJ/cm^2, (c) 490 mJ/cm^2, and (d) 890 mJ/cm^2. The low fluence exposures show the expansion of the vapor bubble below the metal, under conditions where the metal still retains significant tensile strength.

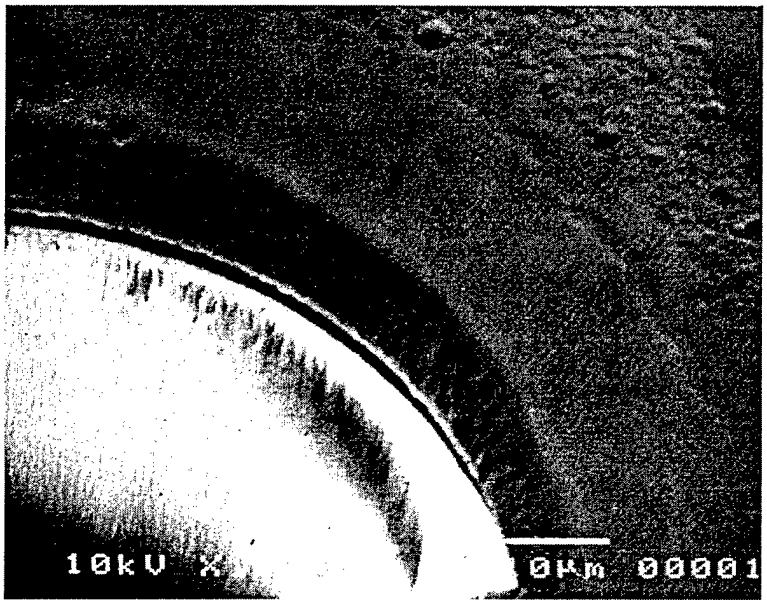

Figure 3: Smoothing of the cathode edge in the conformal mask technique. The illuminated region extends 10 µm past the edge of the well.

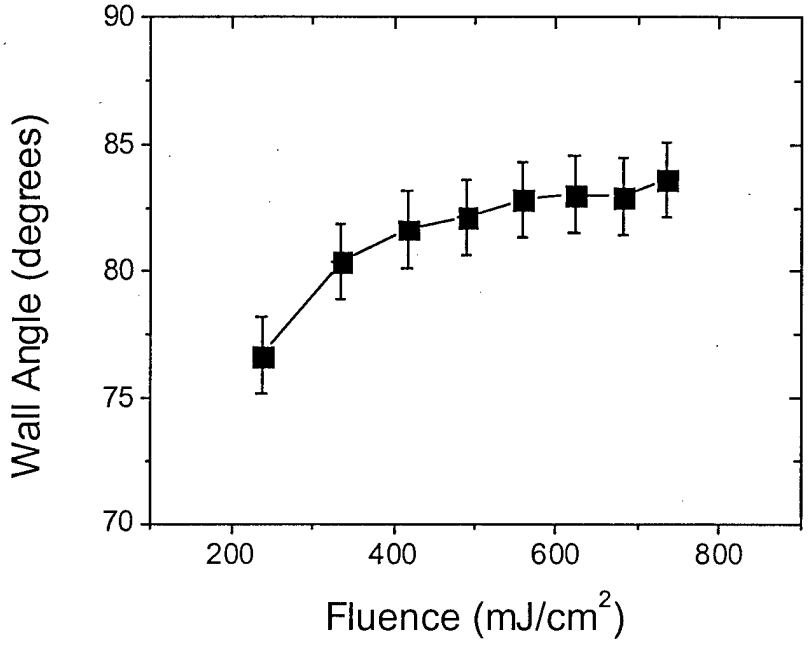

Figure 4: Measured wall angle as a function of laser fluence, showing that the wall angle can be adjusted by suitable choice of machining parameters. The line is drawn to guide the eye.

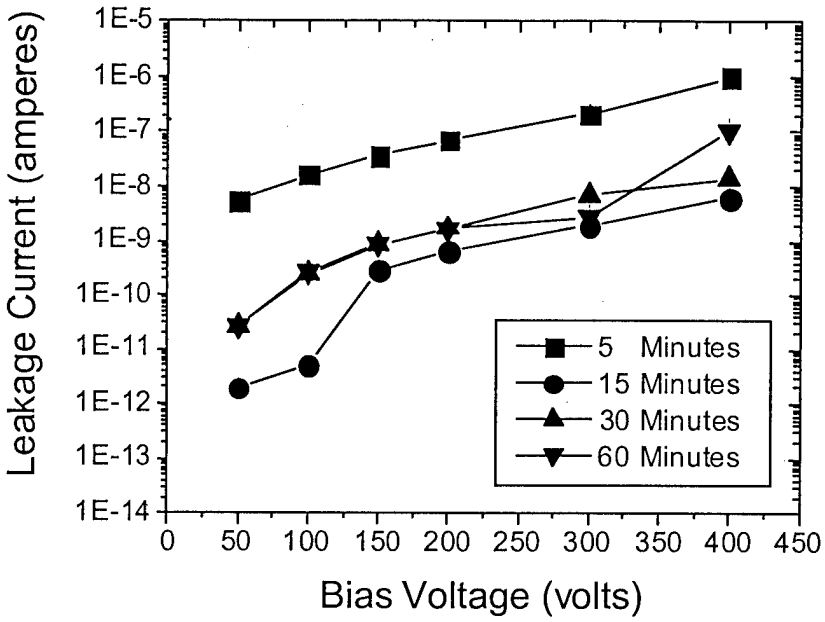

Figure 5: Variation in the leakage current of a 2×2 cm^2 MWD array as a function of exposure to the oxygen plasma cleaning process. The lines are drawn to guide the eye.

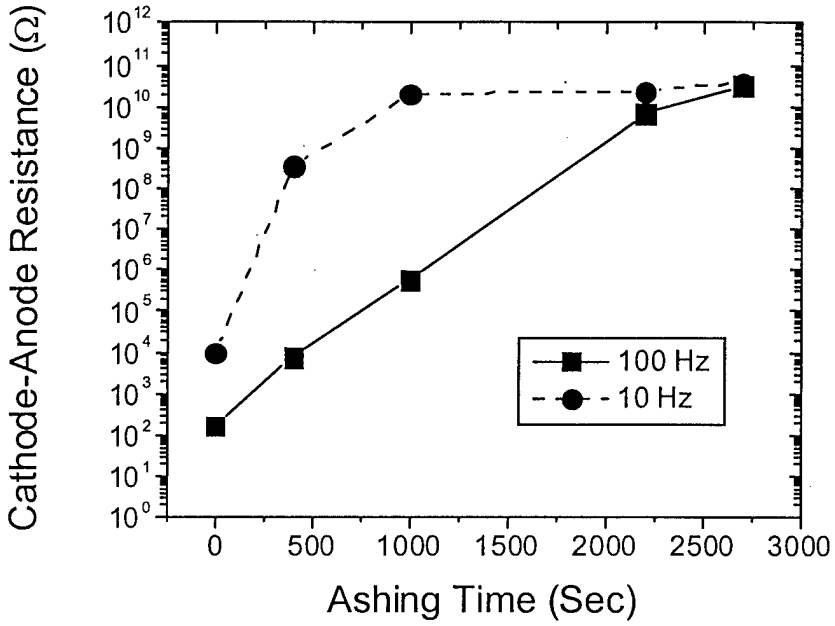

Figure 6: Effect of increasing the laser pulse rate upon internal MWD conductivity. Note that slower machining rates result in much lower internal resistance, indicative of thermal damage to the underlying material. The lines are drawn to guide the eye.